A Novel Profluorescent Nitroxide as a Sensitive Probe for the Cellular Redox Environment

*Benjamin J. Morrow[1], Daniel J. Keddie[1], Nuri Gueven[2], Martin F. Lavin[2], Steven E. Bottle[1]**

[1] ARC Centre of Excellence for Free Radical Chemistry
School of Physical and Chemical Sciences
Queensland University of Technology
GPO Box 2434, Brisbane, Q 4001, Australia

[2] The Queensland Institute of Medical Research,
PO Royal Brisbane Hospital,
Herston, Queensland, 4029, Australia

Address Correspondence to:

Steven E. Bottle
ARC Centre of Excellence for Free Radical Chemistry
School of Physical and Chemical Sciences
Queensland University of Technology
GPO Box 2434, Brisbane, Q 4001, Australia
s.bottle@qut.edu.au

Abstract

Changes to the redox status of biological systems have been implicated in the pathogenesis of a wide variety of disorders. Sensitive quantification of these changes has been developed using a novel fluorescent probe containing a redox-sensitive nitroxide moiety. As well as being able to selectively detect superoxide radical *in vitro*, overall changes to the cellular redox environment can be measured using flow cytometry on the basis of nitroxide reduction. The reversible nature of the probe's detection mechanism offers the unique advantage of being able to monitor redox changes in both oxidising and reducing directions in real time.

Key words: nitroxide, oxidative stress, fluorescent probe

An excess of pro-oxidants in a biological system can lead to the damage of vital cellular components such as proteins, lipids and DNA. Such an imbalance in the redox environment [1] of a cell is described as oxidative stress, and has been implicated in a variety of disorders including cancer, ischemia-reperfusion injury and neurodegeneration [2-4]. Therefore, techniques which are able to quantify and visualise the redox environment of biological systems are crucial tools for investigating links between oxidative stress and disease, and for determining the efficacy of potential antioxidant therapies.

Compounds that have potential in this regard are the stable nitroxide radicals. Nitroxides have been applied as biophysical probes in conjunction with electron paramagnetic resonance (EPR) spectroscopy to monitor properties such as membrane structure [5] and oxygen concentration [6]. They have also found application in monitoring changes in the cellular redox environment on the basis of their metabolism to the reduced hydroxylamines, which are EPR silent. This one electron reduction is the primary metabolic fate of nitroxides, and is dependent on the redox status of the biological system under study [7-12].

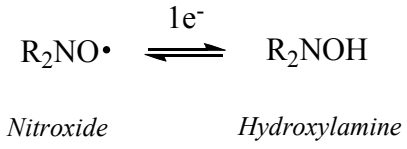

Nitroxide reduction is an intracellular process [9] and is mediated by various reductants such as ascorbate, ubiquinol, tocopherol, and, indirectly, glutathione [9, 11]. In the absence of these reducing equivalents, and in the presence of oxygen, the equilibrium between the oxidised nitroxide molecule and the reduced hydroxylamine

will be shifted towards the more oxidised of the species. Consequently, nitroxide radicals are more persistent in systems under oxidative stress. Since various cellular redox processes are able to mediate conversion between the hydroxylamine and nitroxide species, the ratio of these two states is indicative of the overall 'reducing capacity', or redox environment, of the cell. The reversible nature of hydroxylamine formation adds the important advantage of being able to follow variations in the redox environment of biological systems over time.

Nitroxides have been applied extensively in the field of EPR imaging as *in vivo* probes of redox status, especially in the context of hypoxic tumour environments [11-15]. The characteristic 3-line EPR spectrum of paramagnetic nitroxides can be monitored with time in biological samples. A loss in EPR signal intensity is indicative of hydroxylamine formation, and thus provides a measure of the reducing capacity in these samples. A drawback of this approach is that EPR signal loss may not always arise from hydroxylamine formation. Decreases in nitroxide concentration from the region of interest by some other means, such as excretion, also produces a loss of EPR signal intensity. Furthermore, EPR imaging techniques suffer from limited spatial resolution and are therefore unsuitable to monitor processes occurring at the subcellular level.

An alternative and complementary approach is to use nitroxide probes covalently linked with fluorescent structures possessing excitation and emission profiles of biological relevance. As shown by Blough [16, 17], the covalent linkage of a nitroxide moiety to a fluorophore efficiently quenches the excited states which lead to fluorescence. Reaction of the nitroxide free radical to form a diamagnetic species

removes this quenching effect and thereby leads to a significant increase in the fluorescence yield of the compound. The presence of the nitroxide in these "profluorescent" species thus acts as a redox sensitive on-off switch for the fluorescence of the molecule. In a biological context, this provides a convenient method for distinguishing between relative levels of the diamagnetic hydroxylamine (high fluorescence, reducing conditions) and paramagnetic nitroxide (low fluorescence, oxidising conditions) as a reflection of the redox status of the cell.

Herein, we describe a unique example of a biologically relevant profluorescent nitroxide probe based on the fluorescein class of fluorescent dyes. Fluoresceins possess excellent fluorescence quantum yields, have high water solubility, and have excitation and emission profiles largely free of interference from biological molecules [18]. Incorporating a redox sensitive nitroxide into the fluorescein dye combines these advantages with the potential to probe the cellular redox environment using fluorescence microscopy and flow cytometry. The new nitroxide probe has the significant advantage that the spin is very proximate to the aromatic fluorophore to maximise quenching. By constructing a molecule with the nitroxide built into the fluorescein carbon skeleton, fluorescence arising from fluorophore/spin cleavage is prevented. This novel probe has the potential to provide real-time and reversible responses relating to cellular oxidative stress and the impacts of pro- and anti-oxidants.

Experimental Procedures

Synthesis of 5,6-dibromo-1,1,3,3-tetramethylisoindolin-2-yloxyl (1). To a stirred solution of 5,6-dibromo-1,1,3,3-tetramethylisoindoline **36** (1.3 g, 3.9 mmol) in MeOH (9 mL) and MeCN (370 μL) at room temperature, $NaHCO_3$ (370 mg, 4.4 mmol, 1.1 equiv) and $Na_2WO_4{\cdot}2H_2O$ (150 mg, 0.45 mmol, 0.12 equiv) were added, followed by H_2O_2 (30 %, 3.2 mL, 28.3 mmol, 7.3 equiv). After 120 hours, water (~60 mL) was added to the reaction mixture, which was then extracted with DCM (3 × 60 mL). The combined organics were washed with H_2SO_4 (2M, 2 × 50 mL) and brine (2 × 50 mL), dried (Na_2SO_4) and the solvent was removed under reduced pressure to give a yellow crystalline solid, 5,6-dibromo-1,1,3,3-tetramethylisoindolin-2-yloxyl **21**, (1.19 g, 88 %), which recrystallised from MeCN to give yellow needles (0.93 g, 68 %) mp 254−256 °C (decomp.) (lit. [19] 258 °C); ν_{max} (ATR-FTIR): 3018 (aryl CH), 2976 (alkyl CH), 1468 and 1444 (aryl C-C), 1429 (NO), 638 (aryl C-Br) cm^{-1}. These data agree with those reported previously by Micallef *et al*.[19].

Synthesis of 5,6-dicyano-1,1,3,3-tetramethylisoindolin-2-yloxyl (2). A mixture of 5,6-dibromo-1,1,3,3-tetramethylisoindolin-2-yloxyl **21** (1.75 g, 5.03 mmol), $K_4[Fe(CN)_6]{\cdot}3H_2O$ (868 mg, 2.05 mol, 0.4 equiv, pre-ground), Na_2CO_3 (1.07 g, 10.16 mmol, 2.0 equiv) and $Pd(OAc)_2$ (60 mg, 0.26 mmol, 5 mol%) was heated in DMAC (11 mL) at 130 °C for 3 days. The solution was subsequently poured onto water and extracted with $CHCl_3$. The organic phase was washed with saturated NaCl solution, dried (Na_2SO_4) and the solvent removed under reduced pressure to give crude dinitrile **2** and remaining starting material. Purification by column chromatography ($CHCl_3$) gave 5,6-dicyano-1,1,3,3-tetramethylisoindolin-2-yloxyl **2** (869 mg, 3.62 mmol, 72 %) mp 243-247 °C (lit. [20] 243-248 °C); IR (ATR) ν_{max}: 3039 (alkyl CH), 2979 (aryl

CH), 2231 (CN), 1465(aryl C-C), 1432 (NO) cm^{-1}. These data agree with those reported previously by Barrett *et al*.[20].

Synthesis of 5,6-dicarboxy-1,1,3,3-tetramethylisoindolin-2-yloxyl (3). A suspension of 5,6-dicyano-1,1,3,3-tetramethylisoindolin-2-yloxyl **2** (453 mg, 1.89 mmol) in KOH (2.5 M, 7.5 mL) and absolute ethanol (1.6 mL) was heated at reflux for 16 h. The resultant pale yellow solution was washed with Et_2O (2 × 50 mL), acidified with H_2SO_4 (2M) and extracted with Et_2O (3 × 50 mL). The organic phase was dried (Na_2SO_4) and the solvent removed under reduced pressure to give 5,6-dicarboxy-1,1,3,3-tetramethylisoindolin-2-yloxyl **3** (521 mg, 1.87 mmol, 99 %) mp 246-250 °C (decomp.); ν_{max} (ATR-FTIR): 3545 and 3469 (OH), 2975 (alkyl CH), 2906 (aryl CH), 1705 (C=O), 1432 (NO) cm^{-1}; +EI MS found M^+ 278.10288 (0.11 ppm from calc. mass of $C_{14}H_{16}NO_5^{\bullet}$): *m/z* 278 ($M^+$, 5 %), 260 (65), 245 (38), 230 (100), 215 (82), 171 (50). Recrystallisation from water produced crystals that were of sufficient quality to obtain an x-ray crystal structure (data not shown).

Synthesis of 1,1,3,3-tetramethyl-5,7-dioxo-3,5,6,7-tetrahydro-1H-furano[3,4-f]isoindol-2-yloxyl (4). 5,6-Dicarboxy-1,1,3,3-tetramethylisoindolin-2-yloxyl **3** (610 mg, 2.19 mmol) was refluxed in Ac_2O (10 mL) for 4 h after which a clear orange solution was obtained. Removal of the solvent under reduced pressure gave 1,1,3,3-tetramethyl-5,7-dioxo-3,5,6,7-tetrahydro-1H-furano[3,4-f]isoindol-2-yloxyl **4** (570 mg, 2.19 mmol, 100 %) mp 246-250 °C (decomp.); νmax (ATR-FTIR): 2983 (alkyl CH), 2937 (aryl CH), 1845 and 1776 (C=O), 1621 (aryl C-C), 1442 (NO) cm-1; +EI MS found M+ 260.09340 (4.30 ppm from calc. mass of C14H14NO4•): m/z 260 (M+,

95 %), 245 (50), 230 (97) 215 (100), 171 (80). X-ray quality crystals could be attained by slow crystallisation from Ac_2O (data not shown).

Synthesis of 5-carboxy-6-(6-hydroxy-3-oxo-3H-xanthen-9-yl)-1,1,3,3-tetramethylisoindolin-2-yloxyl (7). Nitroxide anhydride **4** (100 mg, 0.384 mmol) was added to a solution of resorcinol (85 mg, 0.772 mmol, 2 equiv) in $MeSO_3H$ (0.78 mL). The mixture was heated at 85 °C for 24 h and subsequently poured onto ice/water. The solution was treated with NaOH (5 M), to ensure total dissolution of the crude product. The solution was acidified with dropwise addition of conc. HCl and the product was partitioned into Et_2O (3 × 30 mL) and dissolved by addition of MeOH (~20 mL). The solution was filtered to remove insoluble material, dried (Na_2SO_4) and the solvent was removed under reduced pressure, to give the crude product **7**. Purification by column chromatography (20 % EtOH/80 % EtOAc with 0.1 % v/v AcOH), gave **7** as a dark orange crystalline solid (158 mg, 92 %) mp > 300 °C (decomp.); ν_{max} (ATR-FTIR): 3342 (OH), 2977 and 2927 (alkyl CH), 2856 (aryl CH), 1733 (C=O), 1442 (NO) cm^{-1}; +EI MS found M^+ 444.1445 (0.5 ppm from calc. mass of $C_{26}H_{22}NO_6^{\bullet}$): *m/z* 444 ($M^+$, 100 %), 430 (43), 414 (37), 369 (48) 329 (55). See HPLC trace in supporting information.

Synthesis of 5-carboxy-6-(6-hydroxy-3-oxo-3H-xanthen-9-yl)-2-methoxy-1,1,3,3-tetramethylisoindoline (8). A solution of fluorescein nitroxide **7** (20 mg, 0.045 mmol) in DMSO (1.4 cm^3) had $FeSO_4{\cdot}7H_2O$ (25 mg, 0.090 mmol, 2 equiv) and H_2O_2 (30 % aqueous solution, 9 μL) added. The reaction mixture was stirred under argon for 30 min at room temperature after which it was poured onto NaOH (2M, 10 cm^3) and washed with Et_2O (2 × 10 cm^3) and $CHCl_3$ (2 × 10 cm^3) to remove DMSO

present. The aqueous phase was acidified with dropwise addition of conc. HCl and partitioned into Et_2O (30 cm^3) to remove aqueous salts. MeOH (~5 mL) was added to dissolve the product and the mixed solvent removed under reduced pressure to give the crude product. Purification by column chromatography (20 % EtOH/80 % EtOAc with 0.1 % v/v AcOH), gave the fluorescein methyl trap **8** as a dark orange solid (14 mg, 0.030 mmol, 67 %) mp > 300 °C (decomp.); δ_H: (MeOD-d_4); 1.38 (6H, br s, CH_3), 1.54 (6H, br s, CH_3), 3.78 (3H, s, OCH_3), 6.56 (2H, dd, *J* 2.4 and 8.8 Hz, 2'-H and 7'-H), 6.67 (2H, d, *J* 2.4 Hz, 4'-H and 5'-H), 6.72 (2H, d, *J* 8.8 Hz, 1'-H and 8'-H), 7.00 (1H, s, 7-H), 7.78 (1H, s, 4-H); δ_C: (MeOH-d_4); 30.7 (CH_3), 30.8 (CH_3), 66.0 (OCH_3), 68.2 (alkyl C*), 68.6 (alkyl C*), 103.7 (C4' and C5'), 112.6 (C1'a and C8'a), 115.8 (C2' and C7'), 120.1 (C7), 120.5 (C4), 130.9 (C3), 131.1 (C1' and C8'), 131.2 (C8), 149.1 (C4'a and C5'a), 153.8 (C5 and C6), 155.4 (C1), 165.4 (C3' and C6'), 172.2 (C=O); ν_{max} (ATR-FTIR): 3305 (OH), 2962 and 2925 (alkyl CH), 2852 (aryl CH), 1729 (C=O) cm^{-1}; +ESI MS found $(M+H)^+$ 460.174976 (2.3 ppm from calc. mass of $C_{27}H_{26}NO_6^+$): +EI MS *m/z* 459 (M^+, 10 %), 444 (100), 369 (30).

Fluorescence Spectroscopy

Xanthine oxidase from bovine milk (Grade III, ammonium sulphate suspension, 1-2 units/mg protein), hypoxanthine (≥99 %) and diethylenetriamine/nitric oxide adduct (≥97 %) were purchased from Sigma-Aldrich.

Fluorescence measurements were conducted on a Varian Cary Eclipse fluorescence spectrophotometer fitted with a microplate reader accessory. Fluorescein-nitroxide **7** was excited at 492 nm, and the emission detected in the range 492 nm – 600 nm.

Reactions with ascorbate, superoxide and nitric oxide were conducted in 0.01 M phosphate buffered saline, pH 7.4 (PBS). Nitroxide probe **7**, or the alkylated derivative **8**, was added to samples at a final concentration of 1 μM from a 10 mM stock solution prepared in DMSO. Stock solutions of the probes were stored in a -23 °C freezer.

For superoxide assays, 1.4 mg of hypoxanthine was dissolved in 1 mL of 30 mM NaOH solution to make a 10 mM stock solution, which was made fresh prior to each assay. Xanthine oxidase was diluted in PBS just prior to measurement and then added to the reaction solution at a final concentration of 0.03 units/mL.

Nitric oxide assays were conducted using diethylenetriamine/nitric oxide adduct (DETA/NO), which spontaneously releases nitric oxide in aqueous solution [21]. DETA/NO (1.6 mg) was dissolved in 1 mL of 10 mM NaOH solution to give a 10 mM stock solution, which was made fresh prior to each assay. For the oxygen-free experiment, PBS solution containing 1 μM fluorescein-nitroxide **7** was bubbled with N_2 gas for 30 mins and sealed, prior to the addition of DETA/NO solution.

For the reduction of fluorescein-nitroxide **7** with ascorbate, a fresh 0.5 M stock solution of ascorbate was prepared by dissolving ascorbic acid (1.7612 g) and NaOH (0.4000 g) in 20 mL H_2O (pH ≈ 6). Appropriate dilutions were made to achieve a final ascorbate concentration of 100 μM.

Flow Cytometry

Cells (h TERT immortalised fibroblasts) were seeded into a number of separate flasks corresponding to the number of separate treatments (each treatment conducted in triplicate on separate samples) to be performed. They were then cultured in RPMI 1640 growth medium, containing 10 % fetal calf serum and incubated at 37 °C in a 5 % CO_2/air atmosphere. Cells were grown to the required density and then treated accordingly. Nitroxide probe **7**, or the alkylated derivative **8**, was added to all cell samples at a final concentration of 1 μM from a 10 mM stock solution prepared in DMSO. Stock solutions of the probes were stored in a -23 °C freezer.

For 2DG treated cells, a fresh 2 M stock solution was prepared in 0.1 M phosphate buffered saline, pH 7.4. Addition of 2DG to cells were made to give final concentrations of 1 mM, 10 mM and 20 mM. These cells were incubated in the presence of 2DG for 4 hours.

For ROT treated cells, a fresh 100 mM stock solution was prepared in DMSO, which was further serial diluted in DMSO to ensure the final concentration of DMSO in treated cells did not exceed 0.1 %. ROT was added to cells and incubated for a period of 30 minutes.

Following the relevant treatment periods, the medium was removed from the cells and washed with PBS (5 mL). Cells were subsequently washed with EDTA (~2 mL) and then incubated in RPMI 1640 growth medium, containing 10 % fetal calf serum and trypsin for 5 minutes to detach cells from the flask. Cells were then collected and centrifuged (1200 *g*, 5 minutes). After discarding the supernatant, the cell pellet was

resuspended in PBS before being centrifuged once more (1200 *g*, 5 minutes). Supernatant was discarded, and the cells were resuspended in PBS and analysed on a Becton Dickinson FACScan flow cytometer. The nitroxide probe **7** was excited using an air-cooled argon laser at 488 nm, and emission was detected at 530 nm. Statistical analysis was conducted on a count of at least 20,000 cells.

Fluorescence Imaging

Cells (h TERT immortalised fibroblasts) were cultured in RPMI 1640 growth medium, containing 10 % fetal calf serum and incubated at 37 °C in a 5 % CO_2/air atmosphere. Stock solutions of the fluorescein-nitroxide probe **7** were made fresh in DMSO at a concentration of 10 mM, which was added to the cells to give a final concentration of 1 μM. After incubation of the cells for 15 minutes, 45 minutes, or 2 hours in the presence of the nitroxide probe **7**, cells were washed three times and then incubated with L-15 media in an incubator stage attached to an Applied Precision Deltavision Deconvolution Microscope.

Results

Synthesis

Synthesis of fluorescein is commonly achieved *via* the condensation of a substituted phthalic anhydride with two equivalents of resorcinol. In order to incorporate the nitroxide functionality within the fluorescein structure, a novel nitroxide-based

phthalic anhydride was synthesised and used as a direct precursor to the final probe molecule (Scheme 1).

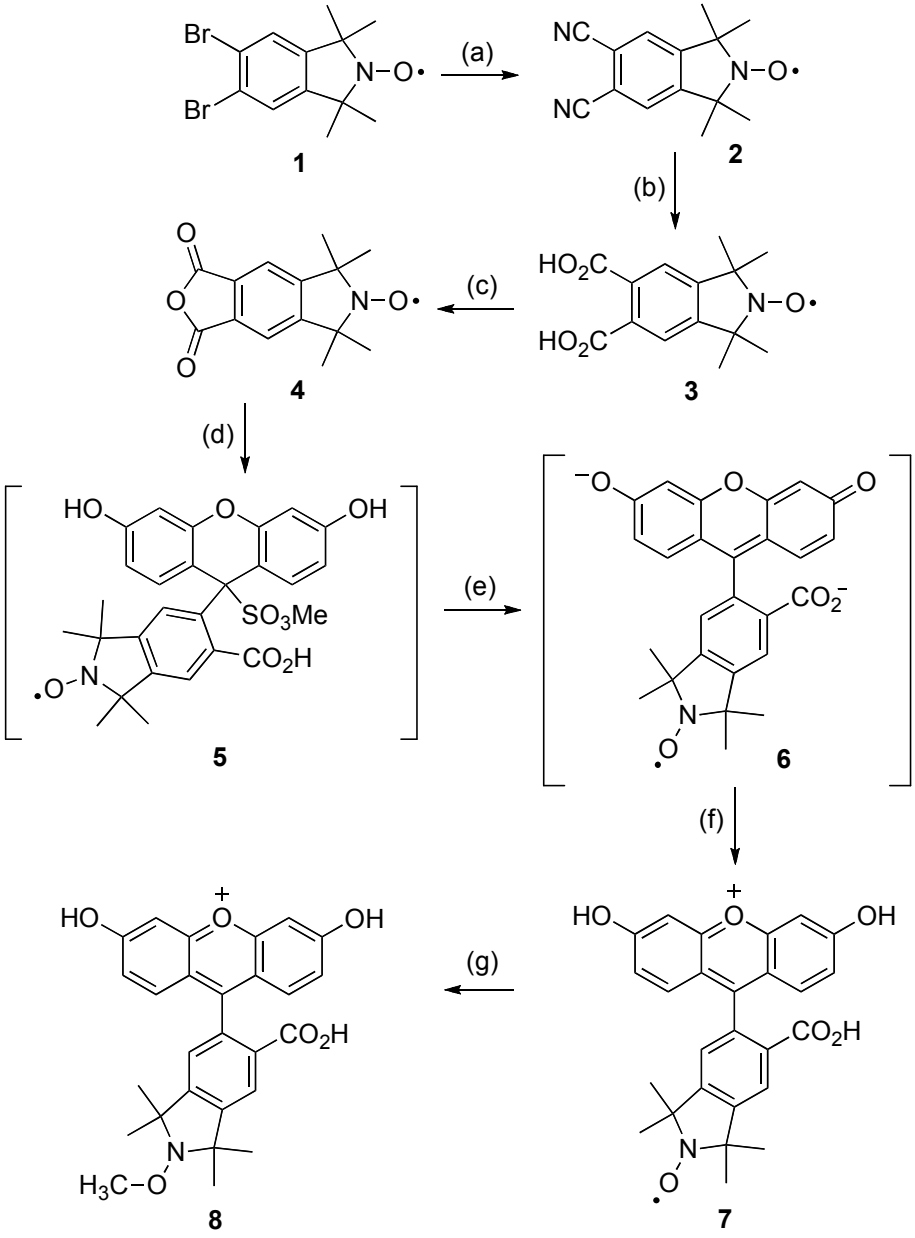

Scheme 1. (a) $K_4[Fe(CN)_6].3H_2O$, $Pd(OAc)_2$, Na_2CO_3, DMAC, 130°C, 72 hrs; (b) KOH, EtOH/H_2O, reflux, 16 hrs; (c) Ac_2O, reflux, 4 hrs; (d) Resorcinol, $MeSO_3H$, 85°C, 24 hrs; (e) NaOH; (f) HCl; (g) $FeSO_4.7H_2O$, H_2O_2, DMSO, RT, 1 hr

The nitroxide anhydride was obtained by cyanation of the previously reported [19] dibromo species **1**, followed by hydrolysis to give the di-carboxy derivative **3**. Subsequent cyclisation in acetic anhydride afforded the nitroxide-substituted phthalic

anhydride **4**. Two equivalents of resorcinol were then combined with **4** in methanesulfonic acid at 85 °C for 24 hours to give the sulfonate ester intermediate **5** [22] which was subsequently treated with NaOH to produce the fluorescein dianion **6**. In aqueous solutions, fluorescein derivatives are known to exist in cationic, neutral, anionic and dianionic forms, each possessing its own absorption and fluorescence characteristics (Scheme 2) [18, 23]. Conversion between these species is a facile process dependent on the pH of the aqueous environment.

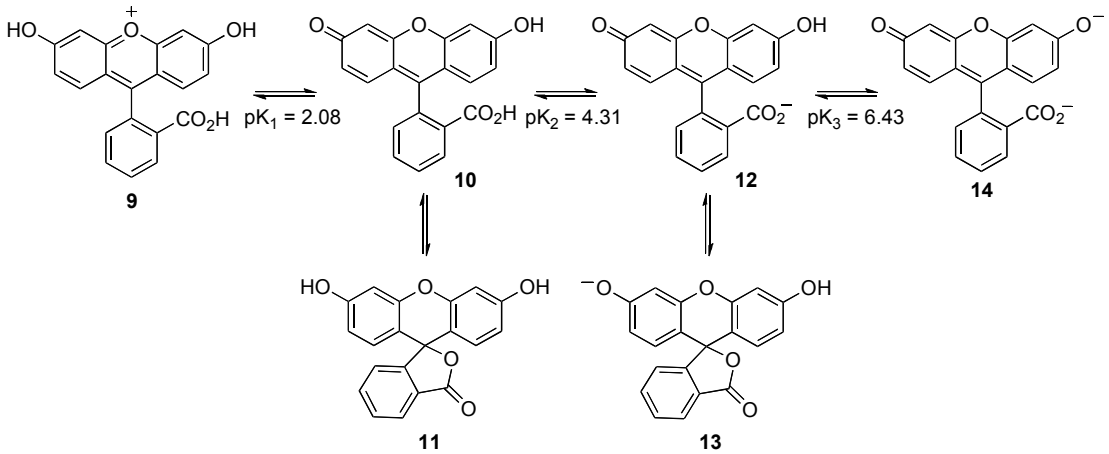

Scheme 2. Protolytic equilibria of fluorescein in aqueous solutions

Although the dianion is the desired fluorescent species, fluoresceins are typically isolated from acidic solution for ease of purification and handling. Thus isolation of the final product was achieved by acidification to precipitate the fluorescein-nitroxide **7**, which, after purification by chromatography, was obtained in 92 % yield. High-resolution mass spectrometry and HPLC facilitated characterisation of the nitroxide probe, however NMR identification was not possible due to the paramagnetic broadening effect of the free radical.

Nitroxide **7** was further derivatised to give the, non-radical, methoxyamine **8** in 67 % yield. As well as being useful for NMR characterisation, this methoxyamine derivative provided a suitable positive control for fluorescence experiments with **7**, due to its structural similarity, but without the nitroxide functionality and fluorescence quenching effect of the free radical. The ^{13}C spectrum confirmed the cationic conformation of the derivative.

In Vitro Spectroscopic Properties and Response to Oxidising/Reducing Species

Due to the pH dependence of the fluorescence of fluorescein-based compounds, the spectra of **7** and **8** (shown in Figure 1) were recorded in 0.1 M NaOH solution, where fluoresceins are highly fluorescent and the quantum yield of the parent compound fluorescein is known [24]. A 1 μM solution of the nitroxide probe **7** in 0.1 M NaOH exhibited relatively weak fluorescence with an excitation wavelength at 492 nm, and an emission maximum at 514 nm. The alkylated, non-radical methoxyamine derivative **8** produced an identical fluorescence profile, but with a significantly higher intensity than that of the nitroxide precursor (Figure 1).

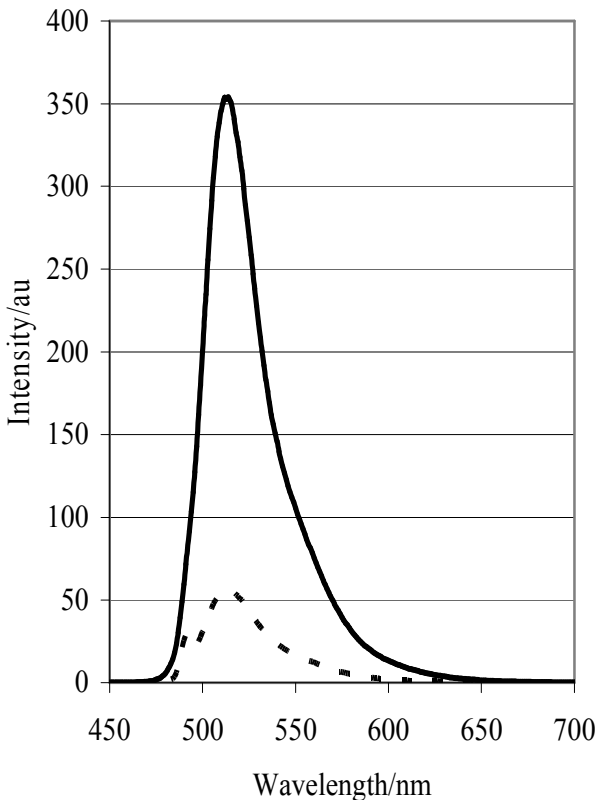

Figure 1. Fluorescence spectra of fluorescein-nitroxide **7** (---) and methoxyamine derivative **8** (—) excited at 492 nm in 0.1M NaOH normalised to 1 μM

Fluorescein (Φ_F = 0.93) [24] in 0.1 M NaOH was used as a standard for the calculation of quantum yields of both nitroxide **7** and methoxyamine **8**. Understandably, the quantum yield of the fluorescein-methoxyamine **8** (Φ_F = 0.93) mirrored that of the unsubstituted fluorescein, while the fluorescein-nitroxide **7** (Φ_F = 0.15) had a considerably lower quantum yield than either of the non-radical derivatives.

Removal of the nitroxide free radical in the novel probe **7** by one-electron reduction to the hydroxylamine resulted in a corresponding increase in fluorescence intensity at 514 nm. This reduction was facilitated by a large excess of hydrazine hydrate (175 mM) in a 1 μM solution of **7** in 0.1 M NaOH. The reversibility of hydroxylamine formation was subsequently demonstrated by vigorous stirring with O_2 present in the

atmosphere, resulting in a concomitant decrease in fluorescence consistent with reformation of the nitroxide radical. This reduction and re-oxidation cycle was repeated twice and demonstrates the ability of the fluorescein-nitroxide probe to dynamically respond to various reductants and oxidants.

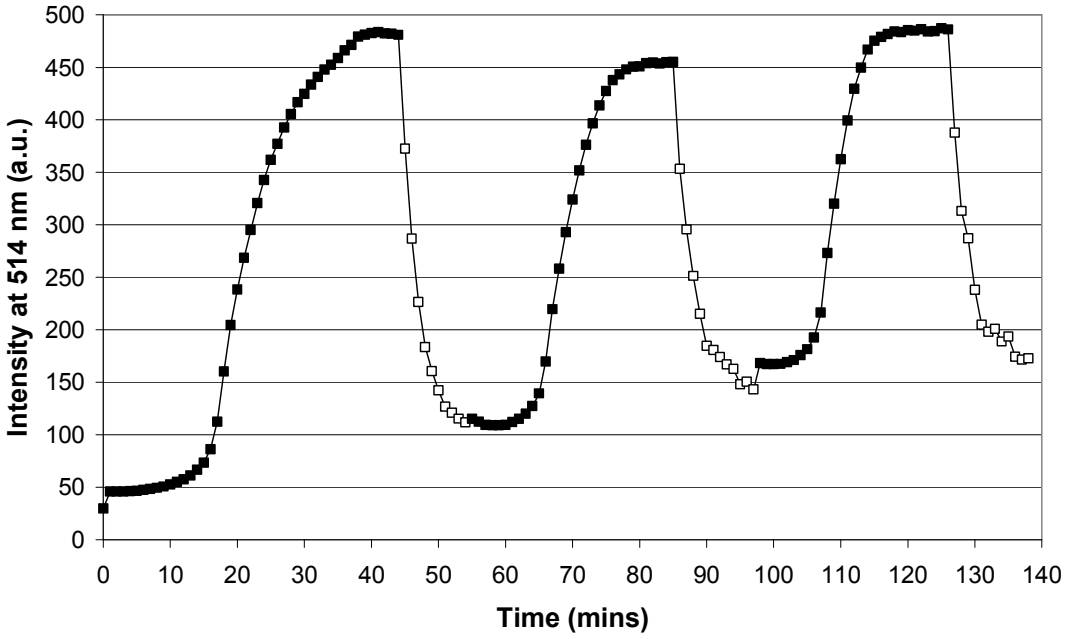

Figure 2. Fluorescence intensity at 514 nm of fluorescein-nitroxide probe **7** in 0.1 M NaOH taken every 1 minute. Dark squares (■) indicate measurements taken without agitation in the presence of a large excess of hydrazine hydrate (175 mM). Data indicated by the light squares (□) were recorded with vigorous mixing in atmospheric oxygen between each measurement.

As previously mentioned, there are a number of pH-dependent protolytic conformations available to fluorescein derivatives, each possessing their own absorption and fluorescence characteristics. As such, the fluorescence properties of the novel probes **7** and **8** are also pH-dependent (see Supporting Information). At biological pH, there is a smaller change in fluorescence between the nitroxide radical derivative and its diamagnetic analogue as compared to the same measurements conducted in a highly basic environment. Thus reduction of nitroxide probe **7** with a

biologically relevant reductant such as ascorbate produced a 2.2-fold increase in fluorescence at neutral pH. This process of hydroxylamine formation is the primary metabolic fate of nitroxides *in vivo*, with a fluorescence increase reflecting a primarily reducing environment. (Figure 3).

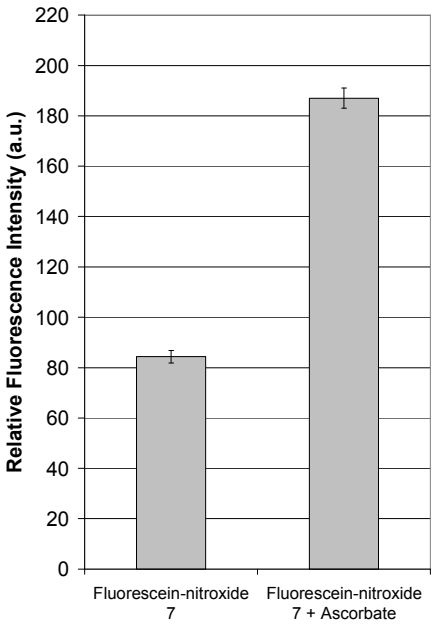

Figure 3. Fluorescence response of the fluorescein-nitroxide **7** (1 μM) following reaction with ascorbate (100 μM) after 13 mins in 0.01 M phosphate buffered saline, pH 7.4. Error bars represent the standard deviation of 3 separate samples.

The *in vitro* responses of the fluorescein-nitroxide (**7**) and those of its non-radical, alkylated derivative (**8**) towards biologically relevant pro-oxidants were also evaluated at biological pH (0.01 M phosphate buffered saline, pH 7.4). The pro-oxidants tested included $O_2^{\bullet-}$, H_2O_2, $^{\bullet}OH$ and $NO^{\bullet}$. Notably, superoxide ($O_2^{\bullet-}$) generated by the action of xanthine oxidase on hypoxanthine [25], gave a 2.2 fold increase in fluorescence (Figure 4, Panel A). Similarly, generation of $NO^{\bullet}$ by the

decomposition of diethylenetriamine/nitric oxide adduct (DETA/NO) [21] led to a 2.7-fold fluorescence increase (Figure 4, Panel B).

A

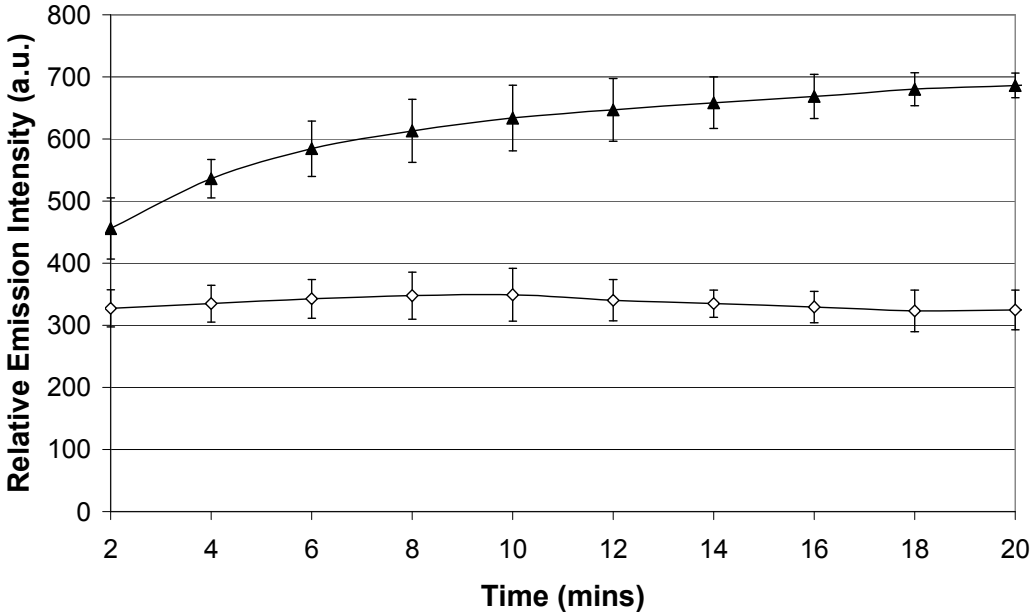

B

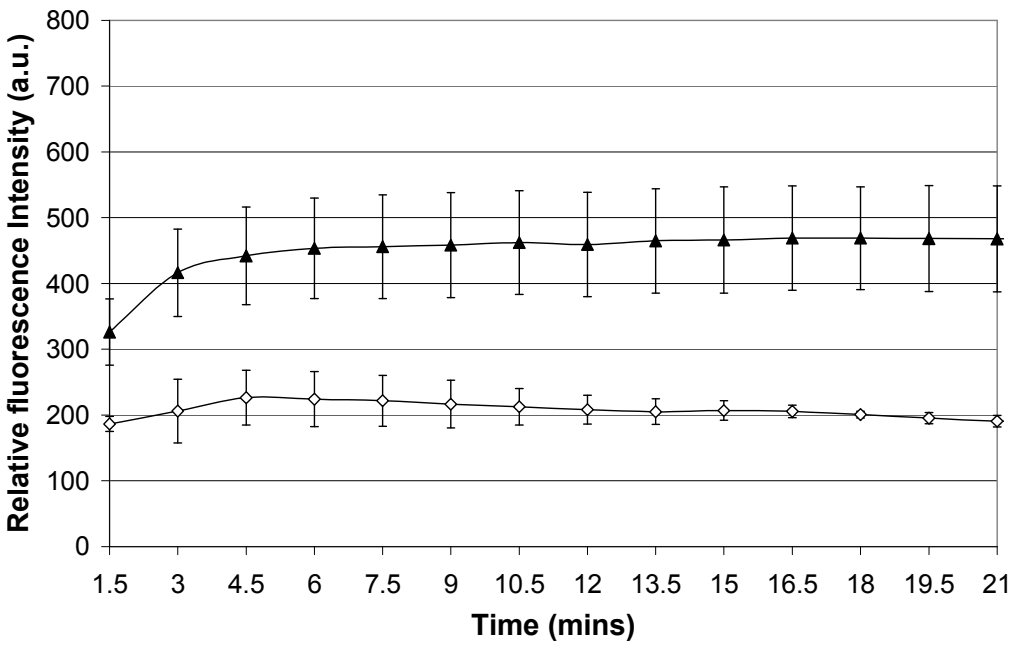

Figure 4. Fluorescence response of the fluorescein-nitroxide **7** to superoxide and nitric oxide. **(A)** Fluorescein nitroxide **7** blank (◇); fluorescein-nitroxide **7** exposed to superoxide generated by the action of 0.03 units/mL of xanthine oxidase on 100 μM hypoxanthine (▲). **(B)** Fluorescein nitroxide **7** blank (◇); fluorescein-nitroxide **7** exposed to nitric oxide released by 500 μM DETA/NO (▲). Measurements taken at a concentration of 1 μM of **7** in 0.01 M phosphate buffered saline, pH 7.4. Each point is the mean of three independent samples (±SD)

However, incubation of the fluorescein-nitroxide **7** with $NO^{\bullet}$ generated by DETA/NO in de-oxygenated buffer produced only a negligible increase in fluorescence output (data not shown). This suggests that the increase seen in air equilibrated buffer (Figure 4, Panel B) probably arises from reaction with higher oxides of nitrogen such as $NO_2^{\bullet}$ and N_2O_3 [26].

The other pro-oxidants tested, H_2O_2 and $^{\bullet}OH$, did not lead to any significant fluorescence response (data not shown). Consequently under these conditions, the probe displays *in vitro* selectivity for superoxide and only responds to $NO^{\bullet}$ via interaction with higher oxide by-products.

To confirm the role of the radical in the fluorescence response for the nitroxide probe, the same assays were conducted using the non-radical alkylated analogue **8**. Exposure of **8** to the redox active species $O_2^{\bullet-}$, H_2O_2, $^{\bullet}OH$ and $NO^{\bullet}$ resulted in no change in the fluorescence detected at 514nm (results not shown). This demonstrates the chemical stability of the fluorophore with respect to these species, and confirms that loss of the nitroxide spin is responsible for the fluorescence increases observed for **7** in response to superoxide and nitric oxide.

Flow Cytometry

The *in vitro* results demonstrate the responsiveness of the fluorescein nitroxide probe **7** towards important redox-active species under relevant biological conditions. In a cellular context however, the nitroxide probe is less likely to have direct interaction with these species due to their low steady state concentrations compared to the intracellular reducing agents which facilitate bioreduction to the hydroxylamine. Thus, while there is an increase in the fluorescence of the nitroxide **7** in response to superoxide itself, it is the overall redox environment, or reducing capacity, of a cell – to which levels of radicals such as superoxide will contribute – which is the most important variable contributing to the fluorescence of **7** in biological samples.

Fibroblasts exhibiting a normal phenotype were immortalised with h TERT and used as a convenient vehicle for studying the cellular redox status under normal physiological conditions. In proliferating h TERT immortalised fibroblasts, incubation with the nitroxide probe **7** for 45 minutes produces a single population at high fluorescence - reflecting complete reduction of the nitroxide to the more fluorescent hydroxylamine (Figure 5, Panel A). Conversely, a confluent sample of h

TERT immortalised fibroblasts incubated with **7** produces a fluorescence histogram indicating the presence of two cellular populations. The population of cells with high fluorescence represents those cells that are able to reduce the nitroxide probe to the highly fluorescent hydroxylamine. The second population possesses much lower levels of fluorescence and represents those cells that retain the probe in its non-reduced nitroxide oxidation state (Figure 5, Panel B).

To confirm that these differences in fluorescence arise from changes in redox state rather than variability in the uptake, retention, excretion or localisation of the fluorophore, analogous samples of h-TERT immortalised fibroblasts were incubated with the alkyl derivative **8** for 45 mins. This compound provides a convenient positive control as it contains the same fluorophore, but without the fluorescence quenching effect and redox sensitivity of the nitroxide species. As expected, these measurements produce a single population at high fluorescence (Figure 5, Panel C). This confirms that the split population measured with **7** in confluent h TERT immortalised fibroblasts arises from differential redox status reflected by different levels of $R_2NO^{\bullet}/R_2NOH$.

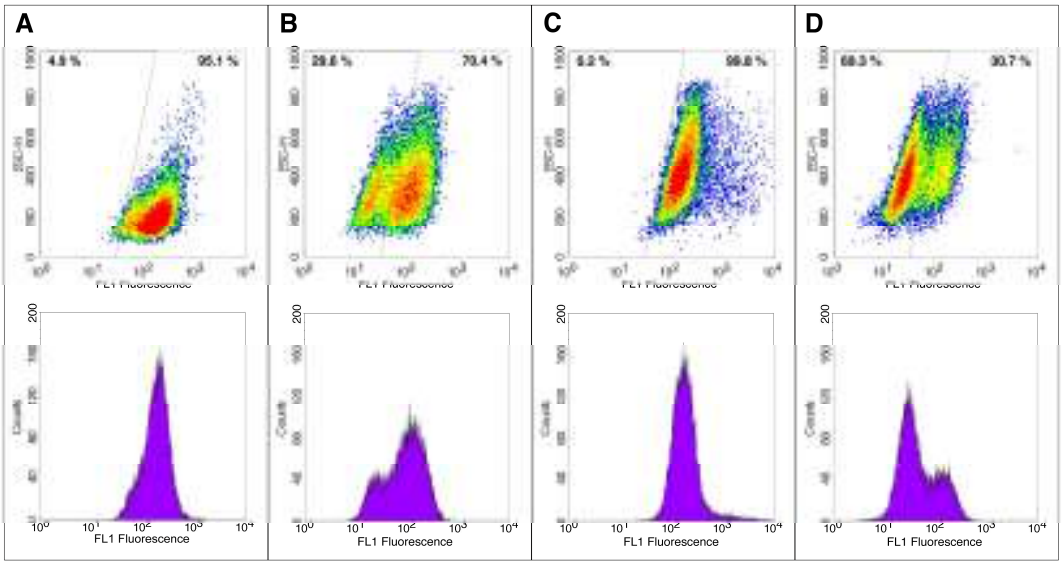

Figure 5. Each panel contains a log density plot of side scatter vs. fluorescence intensity (FL-1, 530 nm), and a histogram of fluorescence intensity (FL-1, 530 nm). **A)** Proliferating h TERT immortalised fibroblasts incubated with **7** (1 μM, 45 mins); **B)** Confluent h TERT immortalised fibroblasts incubated with **7** (1 μM, 45 mins); **C)** confluent h TERT immortalised fibroblasts incubated with **8** (1 μM, 45 mins); **D)** same as in '**B)**' plus treatment with 2DG (20 mM, 4 hours) and ROT (100 nM, 30 mins)

Thus for confluent fibroblasts, the nitroxide probe **7** showcases the different redox environments of the cycling and non-cycling fractions of a cell population. In the cycling population of fibroblasts the primary means of energy production is anaerobic glycolysis, which results in an overall reducing cellular environment [27]. As the fibroblasts become more confluent, a non-cycling population of cells emerges which primarily relies on aerobic respiration as an energy source due to a lack of glucose availability [27]. In this state, there is a shift in the redox potential of these cells to a more oxidised environment (as measured by the glutathione/oxidised glutathione ratio) [28], and the nitroxide probe **7** is retained in its oxidised, less fluorescent form.

As well as identifying these basal differences in the cellular redox environments of cells with varying metabolic activity, the probe is also able to detect redox changes in

the ‘normal’ reducing environment of proliferating cells which are placed under an artificial oxidative stress by metabolic inhibitors such as 2-deoxy-D-glucose (2DG) and rotenone (ROT).

Since redox homeostasis is intimately linked with glucose metabolism [29, 30], 2DG was selected as an appropriate agent to block cellular glycolysis and thus shift the cell to a more oxidising environment. The products of normal glucose metabolism include pyruvate (due to glycolysis) and NADPH (due to the pentose phosphate pathway), both of which are important in regulating the cellular redox environment. Pyruvate, as well as being essential for energy production in the cell as the precursor for acetyl-CoA, can scavenge pro-oxidants such as hydrogen peroxide and other hydroperoxides [31]. NADPH is also vitally important to redox homeostasis as it is the primary source of reducing equivalents for the glutathione/glutathione peroxidase/glutathione reductase system, as well as the thioredoxin/thioredoxin peroxidase/thioredoxin reductase system [32-34].

Rotenone, on the other hand, blocks the activity of NADH dehydrogenase in the mitochondrial electron transport chain and this results in an increase in the production of reactive oxygen species (ROS) [35-37].

Treatment of confluent cultures of h TERT immortalised fibroblasts with either 2DG or rotenone alone, at varying concentrations, showed little change in the cellular redox capacity, that could be indicated by the fluorescein-nitroxide probe **7**. In the case of 2DG treatment, restriction of the supply of NADPH does not significantly alter the cell’s ability to reduce the nitroxide probe to the hydroxylamine. Without an

additional oxidative insult, the alternate reducing equivalents remaining available to the cell are still able to facilitate nitroxide reduction. Similarly, treatment with rotenone at a number of concentrations does not appear to compromise the cellular redox environment. In this case, normal glucose metabolism in the absence of 2DG must still be able to provide and regenerate sufficient reducing equivalents to detoxify increased ROS production and to reduce the nitroxide probe to the hydroxylamine.

When 2DG and ROT are applied in combination however, there is a significant impact on the cellular redox environment as indicated by a decrease in the number of cells able to reduce the nitroxide to the hydroxylamine (Figure 5, Panel D). A loss of available reducing equivalents in the form of NADPH, combined with an increase in ROS production results in the nitroxide probe remaining in the more oxidised, free-radical and therefore less fluorescent form in the majority of cells. This reflects the more oxidised cellular redox environment now present in these cells that has been created by the combined 2DG/ROT treatment. These findings are consistent with a previous study on transformed fibroblasts which showed an increase in cytotoxicity when 2DG and rotenone were used in combination [37], and showcases the capability of the profluorescent nitroxide to probe the oxidative status within the cell.

Flow cytometry shows that the response of the probe to cellular oxidative status occurs in a concentration-dependent manner with respect to 2DG (for a fixed rotenone concentration of 100 nM, Figure 6) and rotenone (for a fixed 2DG concentration of 20 mM, Figure 7).

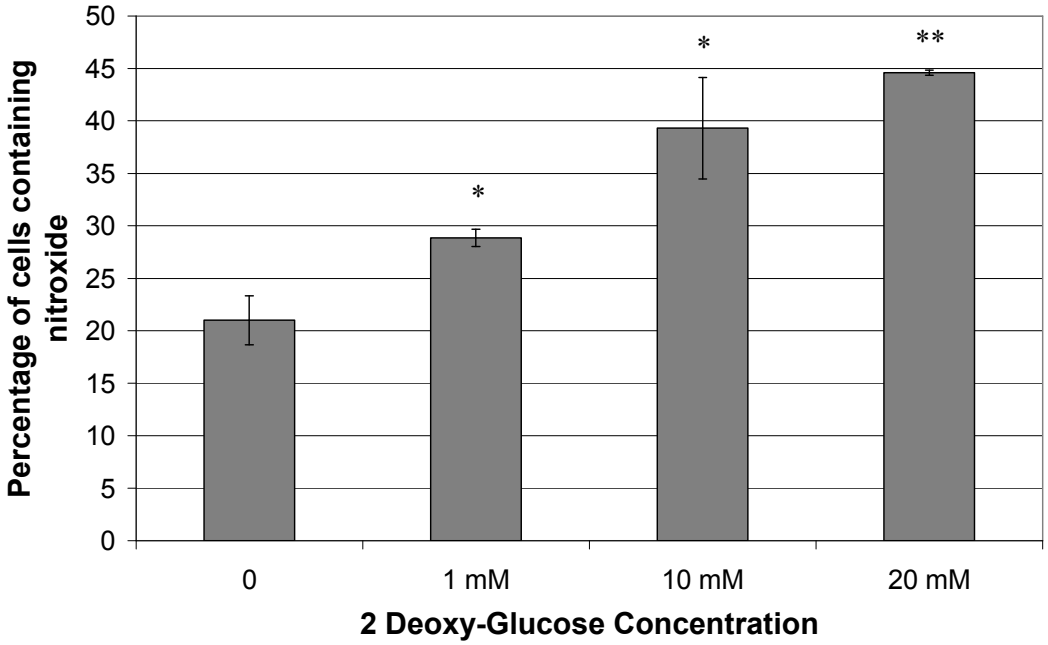

Figure 6. The proportion of cells retaining the oxidised form of the fluorescein-nitroxide probe **7** (at fixed ROT concentration, of 100 nM) is dependent on the concentration of 2DG. Each data point is the mean of three measurements (± SD). Statistical relationship between means determined by two-sample, two-sided *t* tests. *$p < 0.03$ and **$p < 0.01$ vs cells containing no 2DG

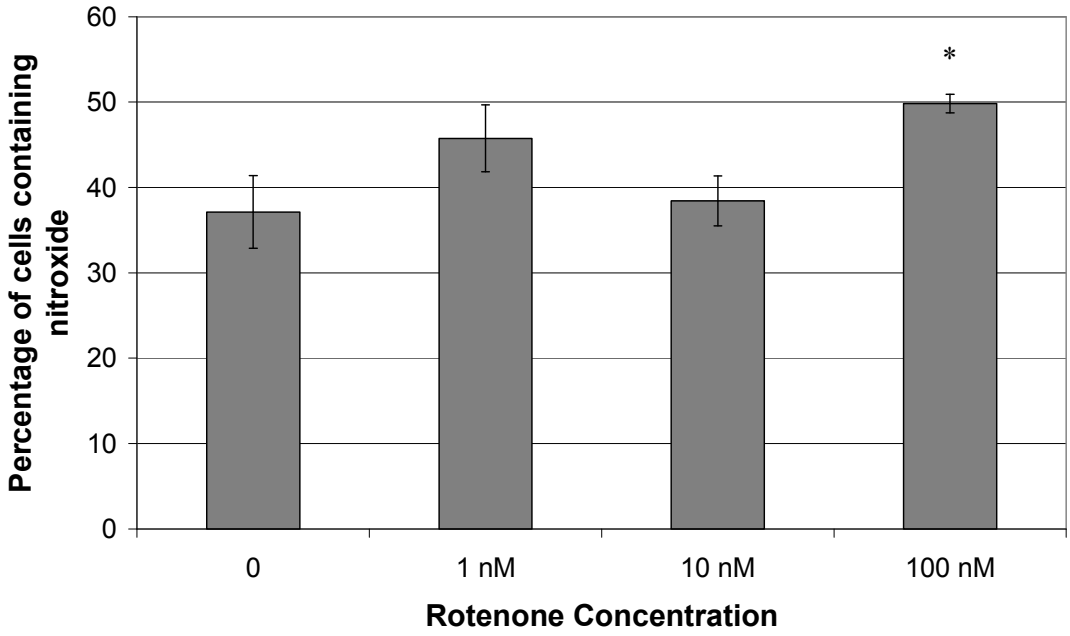

Figure 7. The proportion of cells retaining the oxidised form of the fluorescein-nitroxide probe **7** (at fixed 2DG concentration, of 20 mM) is dependent on the concentration of ROT. Each data point is the mean of three measurements (± SD). Statistical relationship between means determined by two-sample, two-sided *t* tests. *$p < 0.03$ vs cells containing no ROT

Fluorescence Imaging

As well as being well suited to flow cytometry experiments, the emission profile of the fluorescein-nitroxide (**7**) also allows for fluorescent imaging of biological samples. Visualisation of the subcellular regions to which the probe is localising potentially provides insight into the types of oxidative change occurring within cells as indicated by the flow cytometry results. Time-resolved imaging also allows analysis of the mode of uptake of the probe, as well as potentially demonstrating real-time response to further oxidative insult or antioxidant treatment.

In order to assess the mechanism of uptake and metabolism of the probe in normal cells under basal physiological conditions, h TERT immortalised human fibroblasts were incubated with 1 μM of the fluorescein-nitroxide adduct, and visualised after 15 minutes, 45 minutes, and 2 hours (Figure 8).

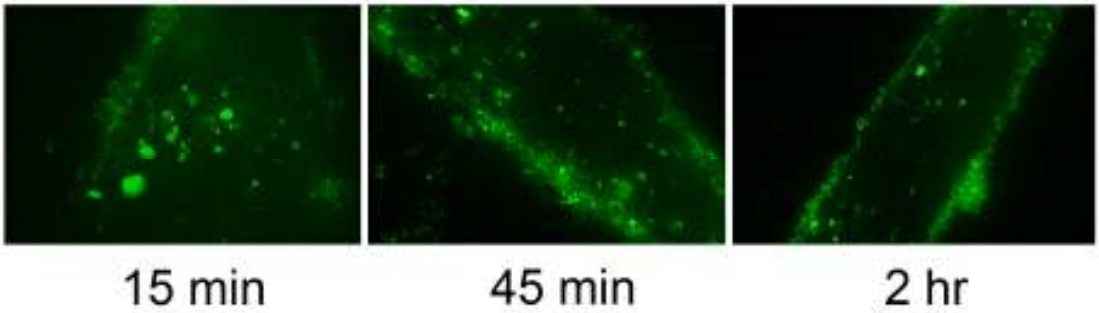

Figure 8. Z-projection of deconvolved image stack of h TERT immortalised human fibroblasts incubated with fluorescein-nitroxide for 15 minutes, 45 minutes, and 2 hours. Cells were washed with L-15 media prior to visualisation.

Following 15 minutes incubation with 1 μM of the fluorescein-nitroxide adduct, fluorescence was observed in the intracellular compartments of the fibroblasts in what appear to be endocytotic vesicles. After 45 minutes incubation time, much of the fluorescent nitroxide probe had migrated from these vesicles to the plasma membrane. This membrane localisation remained apparent after two hours. Although in both the 45 min and the 2 hour incubation time points some of the probe may still be seen in the endosomes, the majority of the material has migrated to the cellular membrane.

In order to ascertain whether these endocytotic vesicles could be identified as, or fuse with, lysosomes at any stage of the incubation period, co-localisation experiments between the nitroxide probe and the commercially available, lysosome-specific probe LysoTracker® Red were undertaken. Both probes were added to the cells

simultaneously and were subsequently visualised after incubation times of 15 mins, 45 mins, and 2 hours as described previously (Figure 9).

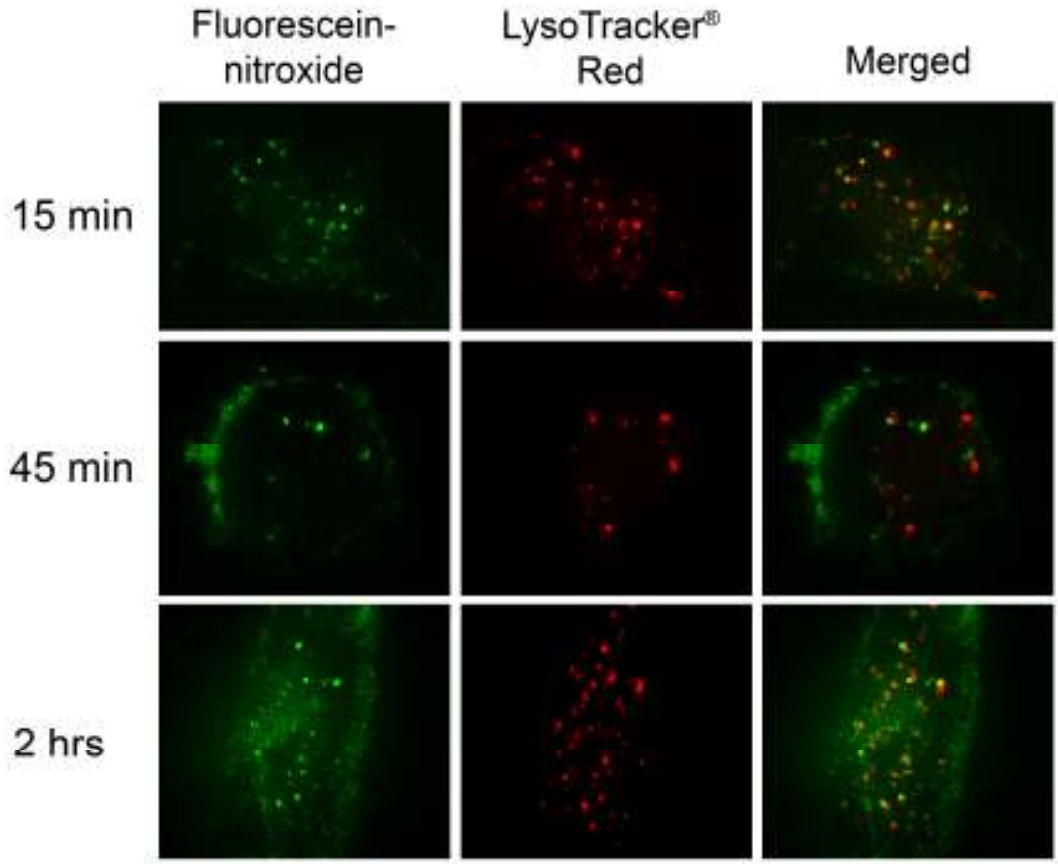

Figure 9. Z-projection of deconvolved image stack of h TERT immortalised human fibroblasts incubated with fluorescein-nitroxide and LysoTracker® Red for 15 minutes, 45 minutes, and 2 hours. Cells were washed with L-15 media prior to visualisation. Left panels show green fluorescence at 528 nm, middle panels show red fluorescence at 617 nm, and the right panels show the merged green and red fluorescence images. Movement of the endocytotic vesicles could be observed in both the red and green channels during live acquisition of image stacks.

As observed previously, the fluorescein-nitroxide probe is initially contained within endocytotic vesicles (15 minutes) before the majority of the probe migrates to the cellular membrane (45 minutes and 2 hours). Co-staining of the lysosomes with LysoTracker® Red in these samples indicates that the vesicles containing the nitroxide probe are co-localising with the lysosomes shown in red. Slight movement of the

lysosomes between the acquisition of each fluorescence channel prevented the direct overlap of the red and green fluorescence as the location of the vesicles were slightly different in each scan.

Discussion

Pro-oxidants are recognised as having a crucial role in various biological processes including the regulation of normal physiological processes [38], as well as contributing to the pathology of conditions such as Alzheimer's disease [39]. In the case of diseases which have been linked to oxidative stress, antioxidant intervention is of potential therapeutic benefit. Therefore, detection of changes to the cellular redox environment as a result of pro-oxidant or antioxidant processes is important for understanding the mechanistic links between free radical chemistry and biological outcomes.

The most effective way to define the mechanistic links between oxidative stress and various cellular processes is with real-time measurement of redox changes occurring in live cells. Fluorescent chemical probes are excellent tools in this regard, since they are able to provide spatial and temporal information with high sensitivity. There are varied examples of such probes in the literature, all of which rely on a 'one-way' detection method. This approach involves non-reversible reaction of a non-fluorescent probe molecule with a radical of interest to produce a detectable fluorescent product. Although challenges relating to probe specificity [40, 41] are being addressed [42, 43], the non-reversible detection approach of this research remains unchanged. The advantage of using a nitroxide as the redox-sensitive element in the fluorescent probe

presented in this work is its ability to reversibly interconvert between the nitroxide and hydroxylamine. Since the ratio of these two states is a measure of the cellular redox environment [8, 11-15], the fluorescein nitroxide probe **7** allows dynamic detection of changes to the oxidative status of biological systems.

Therefore, as well as providing specific detection of superoxide in cell-free systems, the nitroxide probe described here may also serve as a dynamic fluorescent indicator of the overall redox environment in cellular systems, which can be analysed using a variety of analytical techniques such as flow cytometry. Knowledge of the mechanism of uptake and localisation of the probe, as visualised using deconvolution fluorescence microscopy, also provides a powerful tool with which to identify the sites of redox changes occurring inside the cell.

In summary, this new probe and imaging technology provides a reversible and real-time response towards oxidative changes and may allow the testing of antioxidant therapies of potential benefit to a range of diseases linked to oxidative stress.

References:

[1] Schafer, F. Q.; Buettner, G. R. Redox environment of the cell as viewed through the redox state of the glutathione disulfide/glutathione couple. *Free Radical Biol. Med.* **30:**1191-1212; 2001.

[2] Wiseman, H.; Halliwell, B. Damage to DNA by reactive oxygen and nitrogen species: role in inflammatory disease and progression to cancer. *Biochem. J.* **313 (Pt 1):**17-29; 1996.

[3] Hess, M. L.; Manson, N. H. Molecular oxygen: friend and foe. The role of the oxygen free radical system in the calcium paradox, the oxygen paradox and ischemia/reperfusion injury. *J. Mol. Cell. Cardiol.* **16:**969-985; 1984.

[4] Lin, M. T.; Beal, M. F. Mitochondrial dysfunction and oxidative stress in neurodegenerative diseases. *Nature (London, U. K.)* **443:**787-795; 2006.

[5] Berliner, L. J.; Editor *Molecular Biology Series: Spin Labeling, Vol. 2: Theory and Applications.* 1979.

[6] Strzalka, K.; Walczak, T.; Sarna, T.; Swartz, H. M. Measurement of time-resolved oxygen concentration changes in photosynthetic systems by nitroxide-based EPR oximetry. *Arch. Biochem. Biophys.* **281:**312-318; 1990.

[7] Belkin, S.; Mehlhorn, R. J.; Hideg, K.; Hankovsky, O.; Packer, L. Reduction and destruction rates of nitroxide spin probes. *Arch. Biochem. Biophys.* **256:**232-243; 1987.

[8] Swartz, H. M. Use of nitroxides to measure redox metabolism in cells and tissues. *Journal of the Chemical Society, Faraday Transactions 1: Physical Chemistry in Condensed Phases* **83:**191-202; 1987.

[9] Swartz, H. M. Principles of the metabolism of nitroxides and their implications for spin trapping. *Free Radical Res. Commun.* **9:**399-405; 1990.

[10] Kuppusamy, P.; Krishna, M. C. EPR imaging of tissue redox status. *Current Topics in Biophysics* **26:**29-34; 2002.

[11] Kuppusamy, P.; Li, H.; Ilangovan, G.; Cardounel Arturo, J.; Zweier Jay, L.; Yamada, K.; Krishna Murali, C.; Mitchell James, B. Noninvasive imaging of tumor redox status and its modification by tissue glutathione levels. *Cancer Res.* **62:**307-312; 2002.

[12] Yamada, K. I.; Kuppusamy, P.; English, S.; Yoo, J.; Irie, A.; Subramanian, S.; Mitchell, J. B.; Krishna, M. C. Feasibility and assessment of non-invasive in vivo redox status using electron paramagnetic resonance imaging. *Acta radiologica (Stockholm, Sweden : 1987)* **43:**433-440; 2002.

[13] Matsumoto, K.-i.; Hyodo, F.; Matsumoto, A.; Koretsky, A. P.; Sowers, A. L.; Mitchell, J. B.; Krishna, M. C. High-Resolution Mapping of Tumor Redox Status by Magnetic Resonance Imaging Using Nitroxides as Redox-Sensitive Contrast Agents. *Clinical Cancer Research* **12:**2455-2462; 2006.

[14] Kuppusamy, P.; Afeworki, M.; Shankar, R. A.; Coffin, D.; Krishna, M. C.; Hahn, S. M.; Mitchell, J. B.; Zweier, J. L. In vivo electron paramagnetic resonance imaging of tumor heterogeneity and oxygenation in a murine model. *Cancer Res.* **58:**1562-1568; 1998.

[15] Li, H.; He, G.; Deng, Y.; Kuppusamy, P.; Zweier, J. L. In vivo proton electron double resonance imaging of the distribution and clearance of nitroxide radicals in mice. *Magnetic Resonance in Medicine* **55:**669-675; 2006.

[16] Green, S. A.; Simpson, D. J.; Zhou, G.; Ho, P. S.; Blough, N. V. Intramolecular quenching of excited singlet states by stable nitroxyl radicals. *J. Am. Chem. Soc.* **112:**7337-7346; 1990.

[17] Blough, N. V.; Simpson, D. J. Chemically mediated fluorescence yield switching in nitroxide-fluorophore adducts: optical sensors of radical/redox reactions. *J. Am. Chem. Soc.* **110:**1915-1917; 1988.

[18] Sun, W.-C.; Gee, K. R.; Klaubert, D. H.; Haugland, R. P. Synthesis of fluorinated fluoresceins. *J. Org. Chem.* **62:**6469-6475; 1997.

[19] Micallef, A. S.; Bott, R. C.; Bottle, S. E.; Smith, G.; White, J. M.; Matsuda, K.; Iwamura, H. Brominated isoindolines: precursors to functionalized nitroxides. *J. Chem. Soc., Perkin Trans. 2***:**65-72; 1999.

[20] Barrett, A. G. M.; Hanson, G. R.; White, A. J. P.; Williams, D. J.; Micallef, A. S. Synthesis of nitroxide-functionalized phthalocyanines. *Tetrahedron* **63:**5244-5250; 2007.

[21] Keefer, L. K.; Nims, R. W.; Davies, K. M.; Wink, D. A. "NONOates" (1-substituted diazen-1-ium-1,2-diolates) as nitric oxide donors: convenient nitric oxide dosage forms. *Methods Enzymol.* **268:**281-293; 1996.

[22] Ueno, Y.; Jiao, G.-S.; Burgess, K. Preparation of 5- and 6-carboxyfluorescein. *Synthesis***:**2591-2593; 2004.

[23] Sjoeback, R.; Nygren, J.; Kubista, M. Absorption and fluorescence properties of fluorescein. *Spectrochim. Acta, Part A* **51A:**L7-L21; 1995.

[24] Magde, D.; Wong, R.; Seybold, P. G. Fluorescence quantum yields and their relation to lifetimes of rhodamine 6G and fluorescein in nine solvents: improved absolute standards for quantum yields. *Photochem. Photobiol.* **75:**327-334; 2002.

[25] Stadler, I. Oxygen consumption methods: xanthine oxidase and lipoxygenase. *Methods in Molecular Biology (Totowa, New Jersey)* **108:**3-14; 1998.

[26] Goldstein, S.; Samuni, A.; Merenyi, G. Reactions of Nitric Oxide, Peroxynitrite, and Carbonate Radicals with Nitroxides and Their Corresponding Oxoammonium Cations. *Chem. Res. Toxicol.* **17:**250-257; 2004.

[27] McKay, N. D.; Robinson, B.; Brodie, R.; Rooke-Allen, N. Glucose transport and metabolism in cultured human skin fibroblasts. *Biochim. Biophys. Acta, Mol. Cell Res.* **762:**198-204; 1983.

[28] Hutter, D. E.; Till, B. G.; Greene, J. J. Redox state changes in density-dependent regulation of proliferation. *Exp. Cell Res.* **232:**435-438; 1997.

[29] Nelson, D. L.; Cox, M. M. *Lehninger Principles of Biochemistry.* New York: Worth Publishers; 2000.

[30] Mailloux, R. J.; Beriault, R.; Lemire, J.; Singh, R.; Chenier, D. R.; Hamel, R. D.; Appanna, V. D. The tricarboxylic acid cycle, an ancient metabolic network with a novel twist. *PLoS One* **2:**e690; 2007.

[31] Nath, K. A.; Ngo, E. O.; Hebbel, R. P.; Croatt, A. J.; Zhou, B.; Nutter, L. M. alpha -Keto acids scavenge H2O2 in vitro and in vivo and reduce menadione-induced DNA injury and cytotoxicity. *American Journal of Physiology (Cell Physiology)* **268:**C227-C236; 1995.

[32] Tuttle, S. W.; Varnes, M. E.; Mitchell, J. B.; Biaglow, J. E. Sensitivity to chemical oxidants and radiation in CHO cell lines deficient in oxidative pentose cycle activity. *Int. J. Radiat. Oncol., Biol., Phys.* **22:**671-675; 1992.

[33] Coleman, M. C.; Asbury, C. R.; Daniels, D.; Du, J.; Aykin-Burns, N.; Smith, B. J.; Li, L.; Spitz, D. R.; Cullen, J. J. 2-Deoxy-D-glucose causes cytotoxicity, oxidative stress, and radiosensitization in pancreatic cancer. *Free Radical Biol. Med.* **44:**322-331; 2008.

[34] Spitz, D. R.; Sim, J. E.; Ridnour, L. A.; Galoforo, S. S.; Lee, Y. J. Glucose deprivation-induced oxidative stress in human tumor cells: a fundamental defect in metabolism? *Ann. N. Y. Acad. Sci.* **899:**349-362; 2000.

[35] Turrens, J. F.; Boveris, A. Generation of superoxide anion by the NADH dehydrogenase of bovine heart mitochondria. *Biochem. J.* **191:**421-427; 1980.

[36] Li, N.; Ragheb, K.; Lawler, G.; Sturgis, J.; Rajwa, B.; Melendez, J. A.; Robinson, J. P. Mitochondrial Complex I Inhibitor Rotenone Induces Apoptosis through Enhancing Mitochondrial Reactive Oxygen Species Production. *J. Biol. Chem.* **278:**8516-8525; 2003.

[37] Ahmad, I. M.; Aykin-Burns, N.; Sim, J. E.; Walsh, S. A.; Higashikubo, R.; Buettner, G. R.; Venkataraman, S.; Mackey, M. A.; Flanagan, S. W.; Oberley, L. W.; Spitz, D. R. Mitochondrial O2.- and H2O2 Mediate Glucose Deprivation-induced Stress in Human Cancer Cells. *J. Biol. Chem.* **280:**4254-4263; 2005.

[38] Nathan, C. Specificity of a third kind: reactive oxygen and nitrogen intermediates in cell signaling. *J. Clin. Invest.* **111:**769-778; 2003.

[39] Meloni, G.; Sonois, V.; Delaine, T.; Guilloreau, L.; Gillet, A.; Teissié, J.; Faller, P.; Vaák, M. Metal swap between Zn7-metallothionein-3 and amyloid-β-Cu protects against amyloid-β toxicity. *Nat. Chem. Biol.* **4:**366-372; 2008.

[40] Wardman, P. Fluorescent and luminescent probes for measurement of oxidative and nitrosative species in cells and tissues: Progress, pitfalls, and prospects. *Free Radical Biol. Med.* **43:**995-1022; 2007.

[41] Halliwell, B.; Whiteman, M. Measuring reactive species and oxidative damage in vivo and in cell culture: How should you do it and what do the results mean? *Br. J. Pharmacol.* **142:**231-255; 2004.

[42] Lim, M. H.; Xu, D.; Lippard, S. J. Visualization of nitric oxide in living cells by a copper-based fluorescent probe. *Nat. Chem. Biol.* **2:**375-380; 2006.

[43] Miller, E. W.; Tulyathan, O.; Isacoff, E. Y.; Chang, C. J. Molecular imaging of hydrogen peroxide produced for cell signaling. *Nat. Chem. Biol.* **3:**349; 2007.

A. HPLC: **7** separated with 60 % MeOH/40 % H_2O

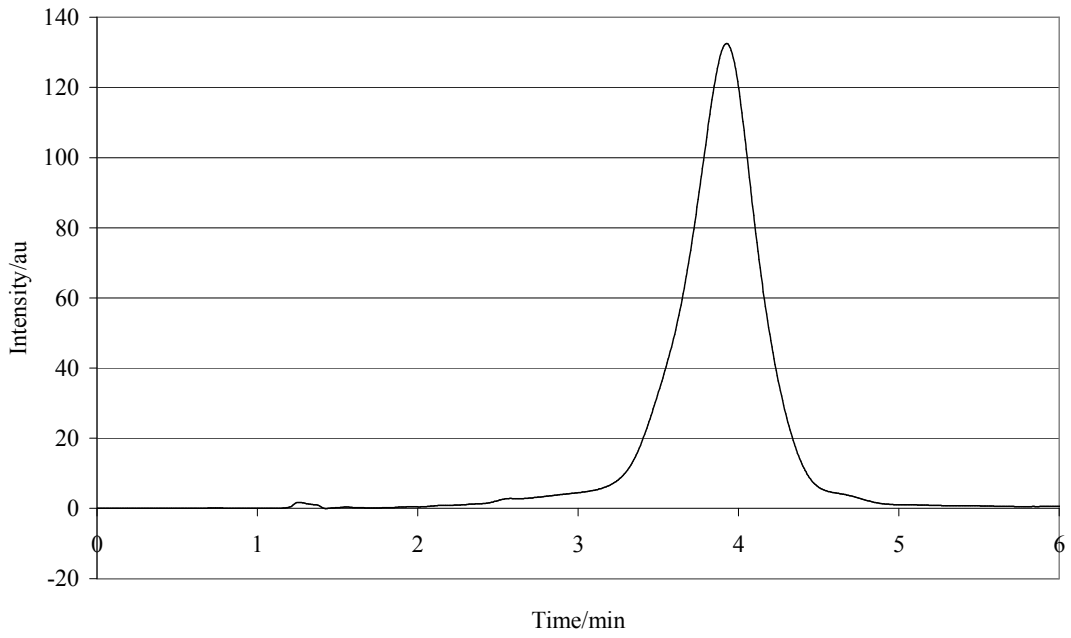

B. The dependence of fluorescence emission intensity of **7** (—) and **8** (—) on pH

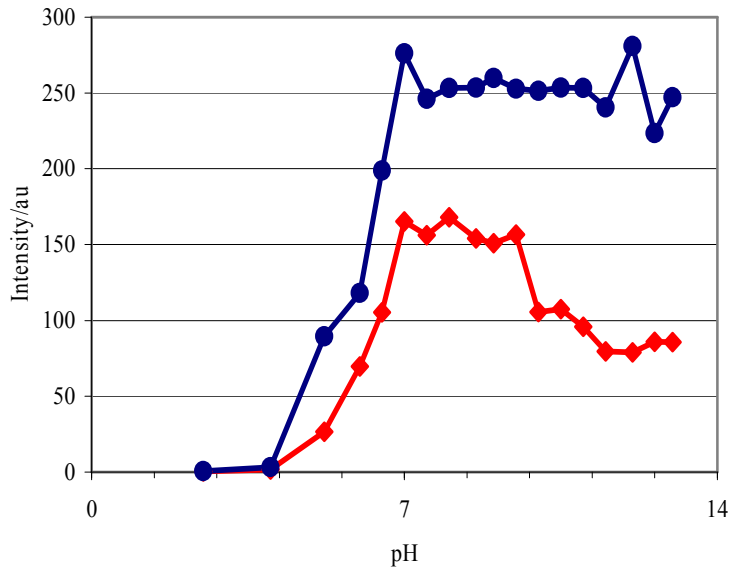

C. HPLC trace of fluorescein-nitroxide probe using fluorescence detector (Excitation: 492 nm, Emission: 514 nm; Solvent A: MeCN + 0.1 % v/v TEAA, Solvent B: H_2O + 0.1 % v/v TEAA; gradient elution over 20 mins of 5:95 Solvent A:Solvent B to 100 % Solvent A)

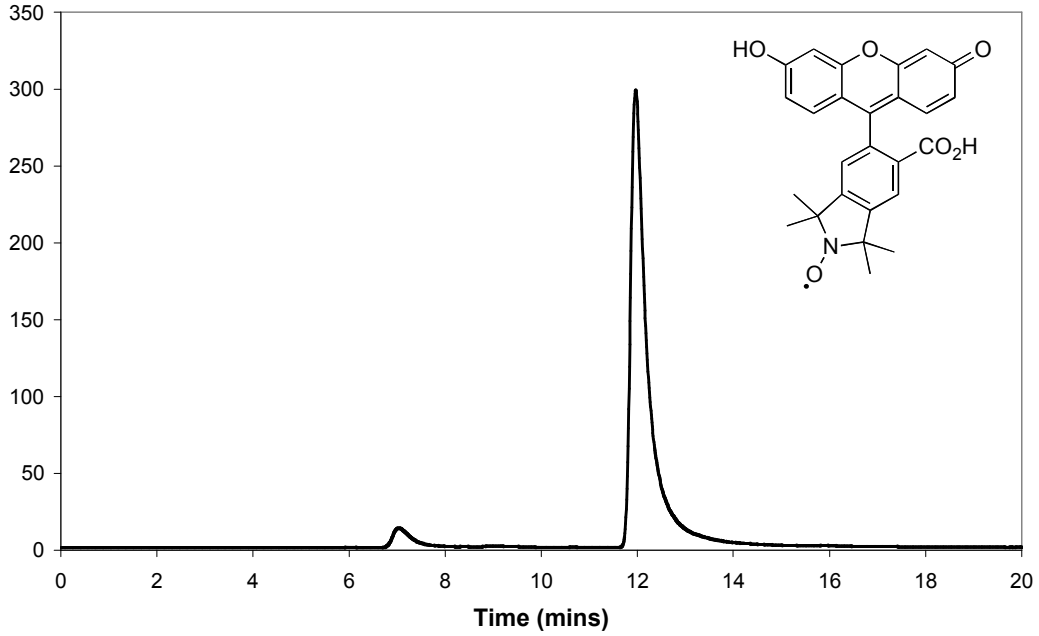

D. HPLC trace of fluorescein-hydroxylamine using fluorescence detector (Excitation: 492 nm, Emission: 514 nm; Solvent A: MeCN + 0.1 % v/v TEAA, Solvent B: H_2O + 0.1 % v/v TEAA; gradient elution over 20 mins of 5:95 Solvent A:Solvent B to 100 % Solvent A)

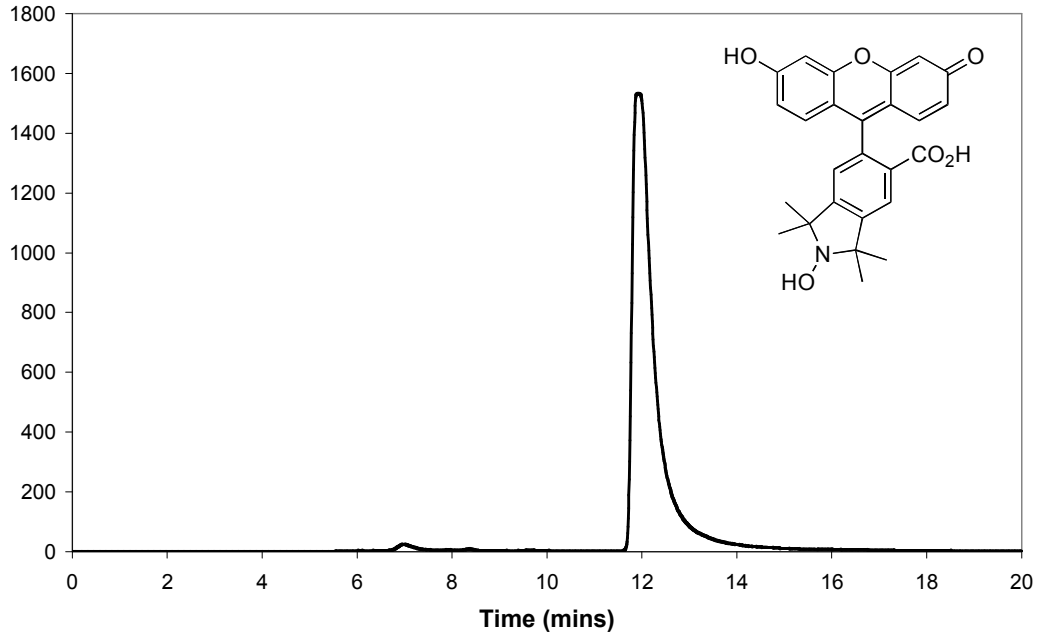

E. NMR spectrum of the fluorescein-hydroxylamine synthesised by hydrogenation with palladium on carbon catalyst (10 %) in MeOH. Once the reaction was complete, the reaction mixture was bubbled with nitrogen for approximately 30 mins to remove most of the MeOH. The crude product was then taken up in deuterated DMSO, filtered through a syringe filter and analysed by ^{1}H NMR spectroscopy.

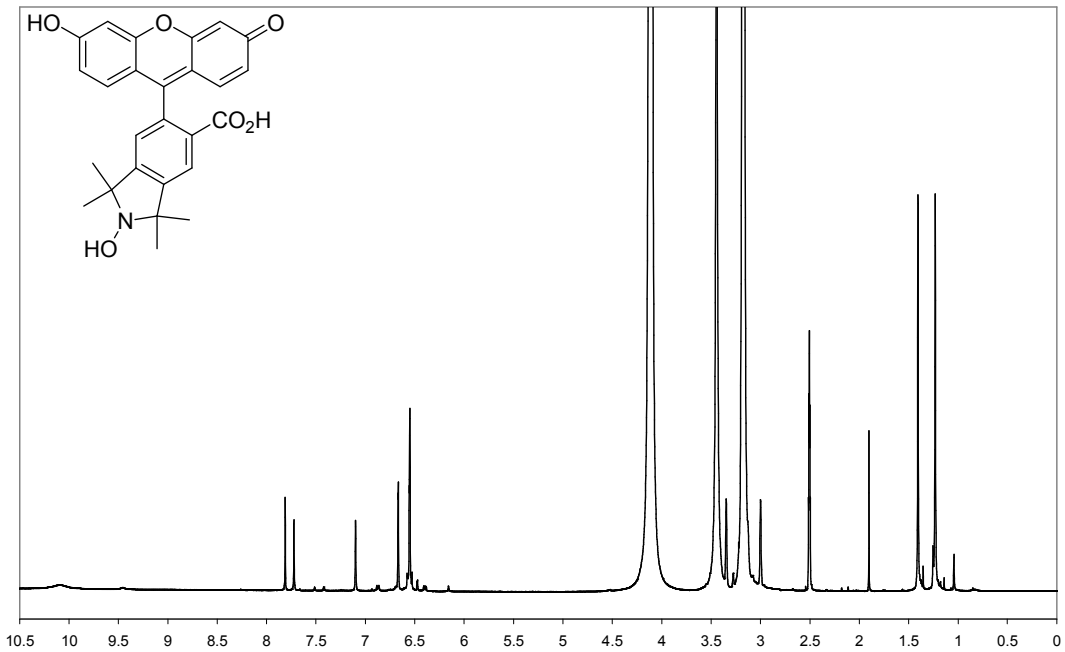

δ_H: (d_6-DMSO); 1.23 (6H, br s), 1.41 (6H, br s), 6.55 (4H, m), 6.68 (2H, s), 7.10 (1H, s), 7.73 (1H, s), 7.82 (1H, s), 10.10 (1H, br). Residual solvent peaks from the filtered crude reaction mixture at 4.12 (OH from MeOH), 3.44 (H_2O), 3.17 (CH_3 from MeOH) and 2.50 (residual DMSO solvent peak).